

RESEARCH ARTICLE

Interplay of phosphate and carbonate ions with flavin photosensitizers in photodynamic inactivation of bacteria

Daniel Bernhard Eckl¹*, Stefanie Susanne Eben¹, Laura Schottenhaml¹, Anja Eichner², Rudolf Vasold³, Andreas Späth⁴, Wolfgang Bäuml², Harald Huber¹

1 Department of Microbiology, University of Regensburg, Regensburg, Germany, **2** Clinic and Polyclinic of Dermatology, University Hospital Regensburg, Regensburg, Germany, **3** Department of Organic Chemistry, University of Regensburg, Regensburg, Germany, **4** TriOptoTec GmbH, Regensburg, Germany

* These authors contributed equally to this work.

* Daniel.eckl@ur.de



OPEN ACCESS

Citation: Eckl DB, Eben SS, Schottenhaml L, Eichner A, Vasold R, Späth A, et al. (2021) Interplay of phosphate and carbonate ions with flavin photosensitizers in photodynamic inactivation of bacteria. *PLoS ONE* 16(6): e0253212. <https://doi.org/10.1371/journal.pone.0253212>

Editor: Adelaide Almeida, Universidade de Aveiro, PORTUGAL

Received: January 22, 2021

Accepted: May 29, 2021

Published: June 11, 2021

Copyright: © 2021 Eckl et al. This is an open access article distributed under the terms of the [Creative Commons Attribution License](https://creativecommons.org/licenses/by/4.0/), which permits unrestricted use, distribution, and reproduction in any medium, provided the original author and source are credited.

Data Availability Statement: All relevant data are within the manuscript and its [Supporting Information](#) files.

Funding: HH and WB received a grand (415812443) from the German Research Foundation (Deutsche Forschungsgemeinschaft DFG; www.dfg.de). The funders had no role in study design, data collection and analysis, decision to publish, or preparation of the manuscript. TriOptoTec GmbH provided support in the form of salaries for the author Andreas Späth, but did not

Abstract

Photodynamic inactivation (PDI) of pathogenic bacteria is a promising technology in different applications. Thereby, a photosensitizer (PS) absorbs visible light and transfers the energy to oxygen yielding reactive oxygen species (ROS). The produced ROS are then capable of killing microorganisms via oxidative damage of cellular constituents. Among other PS, some flavins are capable of producing ROS and cationic flavins are already successfully applied in PDI. When PDI is used for example on tap water, PS like flavins will encounter various ions and other small organic molecules which might hamper the efficacy of PDI. Thus, the impact of carbonate and phosphate ions on PDI using two different cationic flavins (FLASH-02a, FLASH-06a) was investigated using *Staphylococcus aureus* and *Pseudomonas aeruginosa* as model organisms. Both were inactivated *in vitro* at a low light exposure of 0.72 J cm⁻². Upon irradiation, FLASH-02a reacts to single substances in the presence of carbonate or phosphate, whereas the photochemical reaction for FLASH-06a was more unspecific. DPBF-assays indicated that carbonate and phosphate ions decreased the generation of singlet oxygen of both flavins. Both microorganisms could be easily inactivated by at least one PS with up to 6 log₁₀ steps of cell counts in low ion concentrations. Using the constant radiation exposure of 0.72 J cm⁻², the inactivation efficacy decreased somewhat at medium ion concentrations but reached almost zero for high ion concentrations. Depending on the application of PDI, the presence of carbonate and phosphate ions is unavoidable. Only upon light irradiation such ions may attack the PS molecule and reduce the efficacy of PDI. Our results indicate concentrations for carbonate and phosphate, in which PDI can still lead to efficient reduction of bacterial cells when using flavin based PS.

Introduction

Flavins in general are based on a heterocyclic 7,8-dimethylisoalloxazine and appear as yellow substances with excellent water solubility [1,2]. The most important flavin taken up by the

have any additional role in the study design, data collection and analysis, decision to publish, or preparation of the manuscript. The specific roles of the authors are articulated in the “author contributions” section.

Competing interests: Andreas Späth received salaries from the TriOptoTec GmbH. This does not alter our adherence to PLOS ONE policies on sharing data and materials. The other authors have declared that no competing interests exist.

animal digestive tract is riboflavin, also known as vitamin B₂ or as food additive E101 [3]. Unlike riboflavin, FMN (flavin mononucleotide) and FAD (flavin adenine dinucleotide) are commonly associated to proteins as cofactors. The first isolation of a flavin, called lactochrome, was executed in 1879 from cow's milk by the English chemist A. W. Blyth [1,4].

FMN fulfills for example important functions in biochemical pathways [5] as a coenzyme for oxidoreductases [2] and plays a major role in aerobic cellular respiration. FMN functions as an electron carrier in the complex I of the respiratory chain [6]. In addition, flavins play an important role in the bioluminescence of *Aliivibrio fischeri* [7]. In 1949 Arthur W. Galston discovered that riboflavins are capable of oxidizing indolacetic acid in plants by the requirement of oxygen and light, which also led to growth deficits in plants [8].

Flavins are also well known for forming several redox states. They either occur in oxidized form, as semiquinone or hydroquinone. Each redox state of the flavins has a distinct absorbance spectrum that can be used to differentiate between each state [1]. Flavin semiquinones as well as hydroquinones are likely to react with molecular oxygen resulting in the oxidized form that is known to be stable in standard atmospheric condition [1].

The oxidation of flavin molecules via generation of a light-induced triplet state was shown elsewhere [9] as well as singlet oxygen generation of riboflavin [10]. Eichler *et al.* observed that endogenous flavins are capable of producing ROS intracellularly [11]. In this case, the authors could not detect harmful effects and discussed a protective effect of flavin binding proteins. Although such endogenous flavins like riboflavin are capable of efficiently producing singlet oxygen [12–15], a sufficient inactivation of bacteria was not observed [16,17].

The measurement of the quantum efficiency of singlet oxygen generation (Φ_{Δ}) of riboflavin, FMN and FAD by Baier *et al.* in 2006 [14] paved the way for the application of riboflavin as a new photosensitizer (PS) in photodynamic inactivation of microorganisms (PDI).

Thus, the same research group decided to change the disadvantage of riboflavin, namely the lack of a positive net charge hampering the attachment of riboflavin to bacterial cells. The synthesis of cationic riboflavin molecules enabled a highly effective PDI for different bacterial strains [18,19]. A close cell attachment or cellular uptake of a PS is mandatory because singlet oxygen shows a short diffusion range of less than 100 nm in cellular environments [20,21].

Flavins, either cationic or not, are molecules with interesting properties as PS. These molecules are biodegradable and therefore considered safe for human use [18,22]. Limited water solubility hinders gastrointestinal uptake [23] and high doses do not lead to side effects [24]. These properties allow flavins to be used in a wide range of applications ranging from humans to animal products as well as applications in the environment. However, potential fields of application for flavin PS like the human skin, the oral cavity, water disinfection and inanimate surfaces show the presence of different cations such as sodium ions as well as potassium ions and anions like chloride, carbonate and phosphate.

Thus, the present study aimed to investigate PDI with cationic flavin PS, exemplarily regarding the potential impact of sodium carbonate and sodium phosphate in four different concentrations. To unveil the potential effects of such ions, the experiments were performed at low light exposure of 0.72 J cm⁻². Biological logarithmic reduction data were supplemented with assays of PS attachment towards cells, chemical analysis and physical measurements.

Material and methods

Bacterial strains

Bacterial strains were purchased from the German Collection of Microorganisms and cell culture lines (DSMZ, Braunschweig, Germany). As a Gram-positive representative *Staphylococcus*

aureus DMZ 1104 was used, as Gram-negative model organism *Pseudomonas aeruginosa* DSMZ 1117. All organisms were grown on Mueller-Hinton-Agar [25] at 37°C.

Preparation of the ionic solutions

Solutions were prepared as stock solutions with a concentration of 150, 15, 1.5 and 0.15 mmol L⁻¹. As a solvent ultra-pure water with a conductance > 18 Ω was used, hereafter called H₂O. After preparation, solutions were stored in plugged, sealed, gas tight serum bottles under nitrogen atmosphere in the dark at room temperature. pH value was adjusted to 7 with phosphoric acid for sodium phosphate solutions while for sodium carbonate HCl was used for adjustment. Sodium phosphate (Na₃PO₄) was obtained from Merck KGaA, Darmstadt, Germany while sodium carbonate (Na₂CO₃) was bought from Sigma-Aldrich, St. Louis, MO, USA, both in analytical grade.

Photosensitizer

The PS were flavin derivatives designated as FLASH-02a and FLASH-06a [26]. Both PS were purchased from the TriOptoTec GmbH (Regensburg, Germany) with a minimum dye content of 97%. The structure of the PS is displayed in Fig 1A for FLASH-02a and Fig 1B for FLASH-06a, FLASH-02a is a doubly charged cation with a rather small side chain compared with the fourfold charged cationic PS FLASH-06a with remarkably larger side chains. The positive charge of both PS allows the molecules to be located in the vicinity of bacteria enabling efficient inactivation.

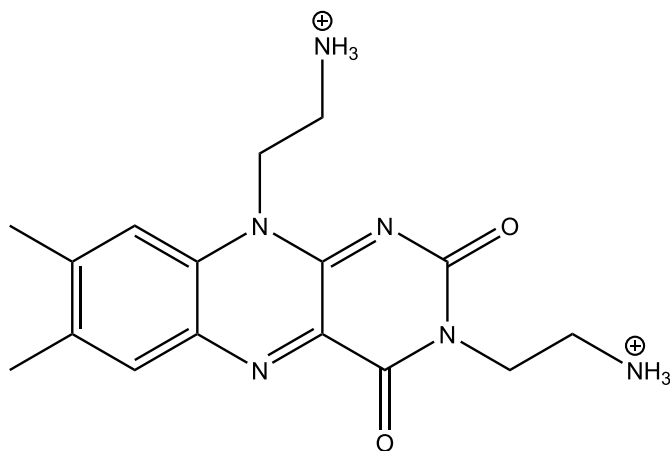
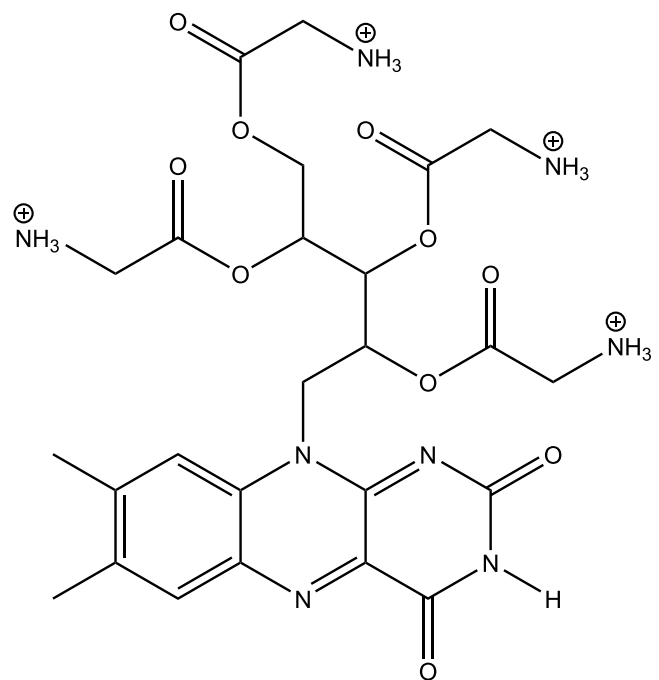
A**B**

Fig 1. Structure of the used PS. (A) shows the structure of FLASH-02a, (B) shows the structure of FLASH-06a. The counterions of the substances were in both cases chloride anions.

<https://doi.org/10.1371/journal.pone.0253212.g001>

Spectroscopy

In order to investigate the chemical interactions of ions and PS at various concentrations, absorption spectroscopy in the visible spectral range (VIS) was performed. Assays were composed out of a total volume of 200 μl with PS concentrations ranging from 0 to 50 $\mu\text{mol l}^{-1}$ and ionic solutions in concentrations of 0.075 mmol l^{-1} to 75 mmol l^{-1} . Spectra measurement took place in 96-well plates utilizing a BMG Labtec plate reader (BMG Labtec, Ortenberg, Germany). Spectra were measured prior and after irradiation with up to 10.8 J cm^{-2} , equivalent to 10 min of irradiation. The obtained percentage transmission was plotted with OriginLab 2019b (Northampton, USA). In order to analyse isosbestic points, the apparent coefficient of variation was calculated as follows

$$CV = \frac{\sigma(\lambda)}{A(\lambda)} \times 100$$

CV: Apparent coefficient of variation

$\sigma(\lambda)$: Standard deviation at wavelength λ

$A(\lambda)$: Absorption at wavelength λ

Whenever an intersection of the spectra occurred and the apparent coefficient was below 2.5% [27], an isosbestic point was assumed.

DPBF-assays

DPBF-assays aimed for a qualitative statement whether the photophysical properties of the dye are hindered in the presence of ions. 1,3-Diphenylisobenzofurane (DPBF) was purchased from Sigma-Aldrich with a minimum dye content of 97%. Each assay was composed as follows: 200 μl in dark 96-well plates (Sarstedt AG & Co. KG, Nuembrecht, Germany) contained a concentration of 0 to 50 $\mu\text{mol l}^{-1}$ PS, 75, 7.5, 0.75 or 0.075 mmol l^{-1} of the corresponding ion and 500 $\mu\text{mol l}^{-1}$ DPBF (dissolved in $\geq 99\%$ methanol, analytical grade). The DPBF solution was prepared immediately before each experiment. Controls consisted out of 100 μl ionic solution in appropriate concentration and 100 μl methanol. Internal references contained 100 μl H_2O and 100 μl methanol with 500 $\mu\text{mol l}^{-1}$ DPBF. Each value for each condition was obtained as the mean value of three independent replicates. The assays were measured after 0, 1, 2, 3, 4, 5 and 10 s of irradiation with the beforehand mentioned light source utilizing a fluorescence plate reader, purchased from BMG Labtech. Excitation wavelength was set to 411 nm while emission was detected at 451 nm. Values obtained for the internal reference were set to 1, relative fluorescence was calculated as ratios to the control and displayed in per cent via OriginLab 2019b. A statistical analysis of the retrieved values was performed afterwards as explained in [S1 File](#).

Light source

Irradiation of all samples was performed with a blue light emitting prototype containing a neon tube with an emission range from about 380–470 nm (BlueV, Medizintechnik Herbert Waldmann GmbH & Co. KG, Villingen-Schwenningen, Germany). Intensity was measured with a thermal sensor (Nova 30 A-P-SH, Ophir-Spiricon, North Logan, UT, USA). All irradiation steps were carried out at a light irradiance of 18 mW cm^{-2} .

Photodynamic treatment of bacteria

Bacteria were taken from the agar plates and suspended in H_2O . Optical density was adjusted to 0.6 at 600 nm utilizing a photometer (Ultrospec 10, Amersham Biosciences, Little Chalfont,

UK). After density adjustment, 1 ml of the bacterial suspension was transferred to 1.5 ml reaction tubes and centrifuged at 13,000 x g for 7 min. Subsequently, supernatant was discarded and the pellet was resuspended in H₂O. Centrifugation was repeated and mixed thoroughly with 1000 µl of ionic solution prepared as mentioned above. 25 µl of the prepared suspension were then mixed with 25 µl of PS-solution in ascending concentrations, incubated for 10 min in absolute darkness and irradiated with a constant energy of 0.72 J cm⁻² (corresponding to an illumination time of 40 s) afterwards.

20 µl of this reacting solution were transferred to 180 µl preheated Mueller-Hinton bouillon and cultivated at 37°C for 48 h. A plate reader measured the optical density at 600 nm which was used to calculate the bacterial reduction as described in detail elsewhere [28]. In principle, the applied method concerning cultivation and evaluation of the microbial reduction is an adaptation of a method initially described by Bechert and co-workers [29] and has been successfully used for example by Bruenke *et al.*[30]. Doubling time was calculated for an optical density of 0.2 and 0.4. All light sensitive parts of the procedure were conducted at low light conditions as investigated elsewhere [31]. Obtained inactivation values, which were obtained from three independent measurements, were analyzed statistically as mentioned in S2–S4 Files.

Binding assays

To investigate binding of flavins to bacteria, optical density at 600 nm was adjusted to 0.6. 500 µl cell suspensions were placed in 1.5 ml reaction tubes, centrifuged as mentioned before and washed in H₂O. The pellet was suspended in 500 µl of ionic solution and 500 µl of PS with a concentration of 100 µmol l⁻¹ and incubated for 10 min in the dark. After incubation, the cells were centrifuged at 4,500 x g for 10 min. The supernatant was transferred into a cuvette and measured against a control. Measurements were carried out at 444 nm for FLASH-02a and 446 nm for FLASH-06a, respectively. Each condition was tested independently thrice leading to three independent values. A statistical analysis of the binding assays was performed and is shown in S5 File.

Statistical analysis

Data from DPBF-assays were collected in three independent replicates, while values of the binding assays and logarithmic reduction rates from the photodynamic inactivation experiments were obtained from three biological replicates of each tested condition. In order to investigate the data statistically the values of the replicates were compared between the tested conditions and p-values were calculated via unpaired, two-tailed t-tests assuming normal distribution. Events were considered statistically significant for p < 0.05. When p was < 0.01, events were considered highly significant, p < 0.001 indicated extremely significant events. The calculated p-values are given in S1–S5 Supporting information, the values of the replicates are given in the S3–S7 Datasets.

Results

Photochemical alterations of the PS

FLASH-02a showed photodegradation upon light exposure as indicated by measuring the transmission of the PS in H₂O after the application of 10.8 J cm⁻² (equal to 10 min of irradiation), equivalent to a loss of concentration of about 17% (Fig 2A). The presence of phosphate and carbonate ions in solutions caused an alteration of the spectra depending on ion concentration and irradiation time. The photochemically changed flavins show isosbestic points at 339 nm (CV = 1.55%), 389 (CV = 0.96%), 440 (CV = 2.25%) and 503 nm (CV = 1.24%) for

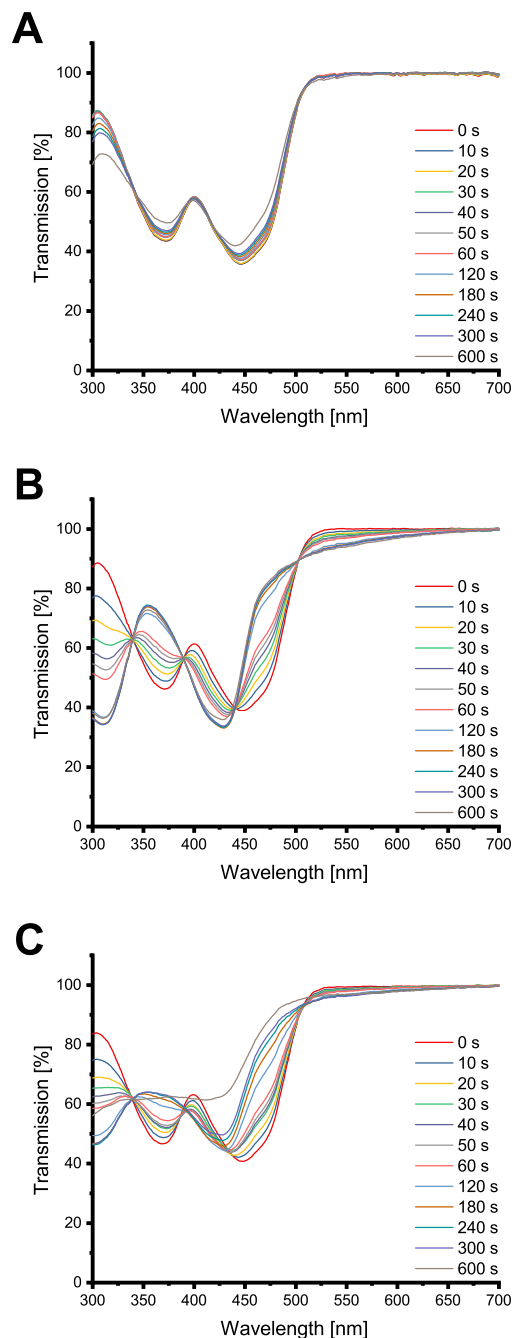


Fig 2. Transmission spectra of FLASH-02a. Y axes indicate the transmission in per cent, x axes the wavelength in nm. Various colors of the spectra indicate different irradiation times. (A) shows the results for H₂O, (B) for 75 mmol l⁻¹ sodium phosphate and (C) for 75 mmol l⁻¹ sodium carbonate.

<https://doi.org/10.1371/journal.pone.0253212.g002>

phosphate (Fig 2B) and 339 nm for carbonate with CV equal to 1.01% (Fig 2C). The acquired transmission data are listed in detail in the S1 Dataset.

FLASH-06a was far more affected by photobleaching most likely due to its large side chains. After the application of 10.8 J cm⁻² (equal to 10 min of irradiation), around 34% of the PS were degraded in the water control (Fig 3A). FLASH-06a in combination with phosphate showed

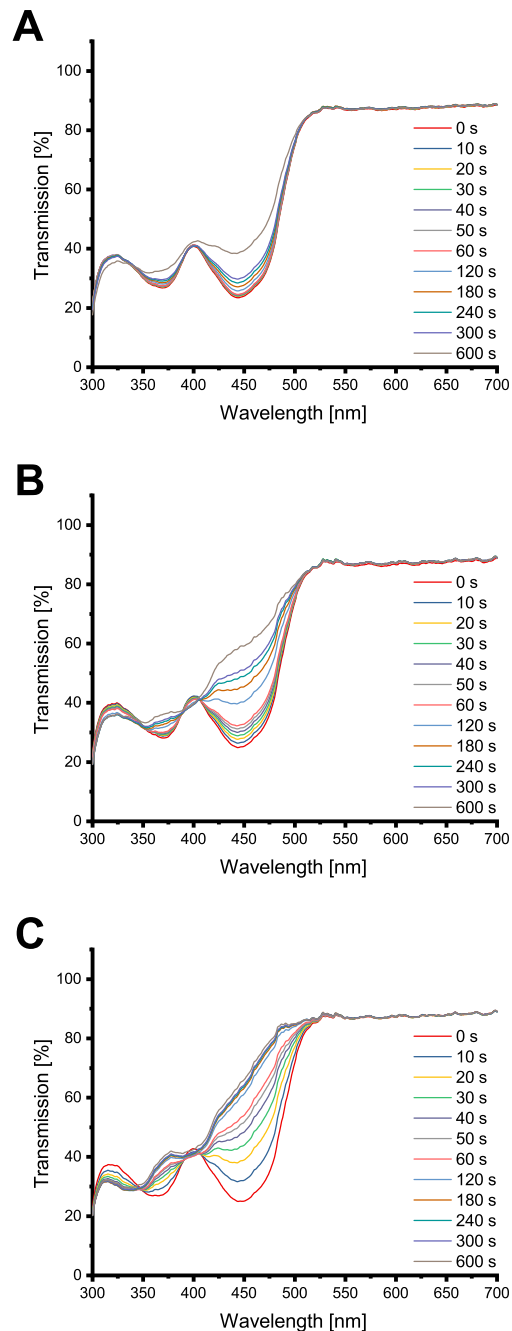


Fig 3. Transmission spectra of FLASH-06a. Y axes indicate the transmission in per cent, x axes the wavelength in nm. Various colors of the spectra indicate different irradiation times. (A) shows the results for H₂O, (B) for 75 mmol l⁻¹ sodium phosphate and (C) for 75 mmol l⁻¹ sodium carbonate.

<https://doi.org/10.1371/journal.pone.0253212.g003>

isosbestic points at 348 (CV = 1.24%), 389 (CV = 0.68%) and 405 nm (CV = 0.83%) (Fig 3B). Interestingly, the isosbestic points for carbonate were about the same wavelength as for phosphate with 346 nm (CV = 1.17%), 393 nm (CV = 1.75%) and 402 nm (CV = 1.95%) (Fig 3C). However, chemical reaction was more pronounced with less light exposure for carbonate. The transmission data are shown in the S2 Dataset.

Singlet oxygen production with and without ions

The singlet oxygen production was monitored by relative fluorescence of DPBF. Without the addition of ions, relative DPBF fluorescence decreased after 10 s of irradiation with 18 mW cm⁻² (equal to 0.18 J cm⁻²) and reached values below 1% for the maximum concentration of 50 μmol l⁻¹ FLASH-02a (Fig 4A). The results for the H₂O control of the DPBF assays carried out with FLASH-02a diverge all significantly from each other—except for a comparison of the highest two PS concentrations (detailed results are displayed in S1 File).

However, with increasing concentrations of sodium phosphate or sodium carbonate, less singlet oxygen was generated as indicated by the constant relative DPBF fluorescence. The statistical analysis also showed in nearly all compared conditions non-significant events, whereas the detailed results are given in S1 File. When using FLASH-06a without the addition of ions, relative DPBF fluorescence decreased after 10 s of irradiation with 18 mW cm⁻² (0.18 J cm⁻²) and reached minimum values below 7% for the maximal concentration of 50 μmol l⁻¹ FLASH-06a (Fig 4B). Again, a comparison of all tested conditions showed that all values were significantly distinct from each other, with the comparison of the highest two PS concentrations being the only exception. With increasing concentrations of sodium phosphate, less singlet oxygen was generated. However, the obtained values for 1 and 5 μmol l⁻¹ of FLASH-06a differ from the other PS concentrations significantly (S1 File). The same result was observed for increasing concentrations of sodium carbonate, in which none of the tested conditions does vary significantly from each other (S1 File). Values above 100% indicate that the photobleaching effect due to residual light of the control exceeded the decrease in fluorescence caused by singlet oxygen production of the photosensitizer. Measured values, means and standard deviation are shown in the S3 Dataset.

Photodynamic inactivation of bacteria with and without ions

PDI experiments in H₂O revealed a higher inactivation efficiency for *Pseudomonas aeruginosa* (Fig 5C and 5D) compared to *Staphylococcus aureus* for both PS (Fig 5A and 5B). In general,

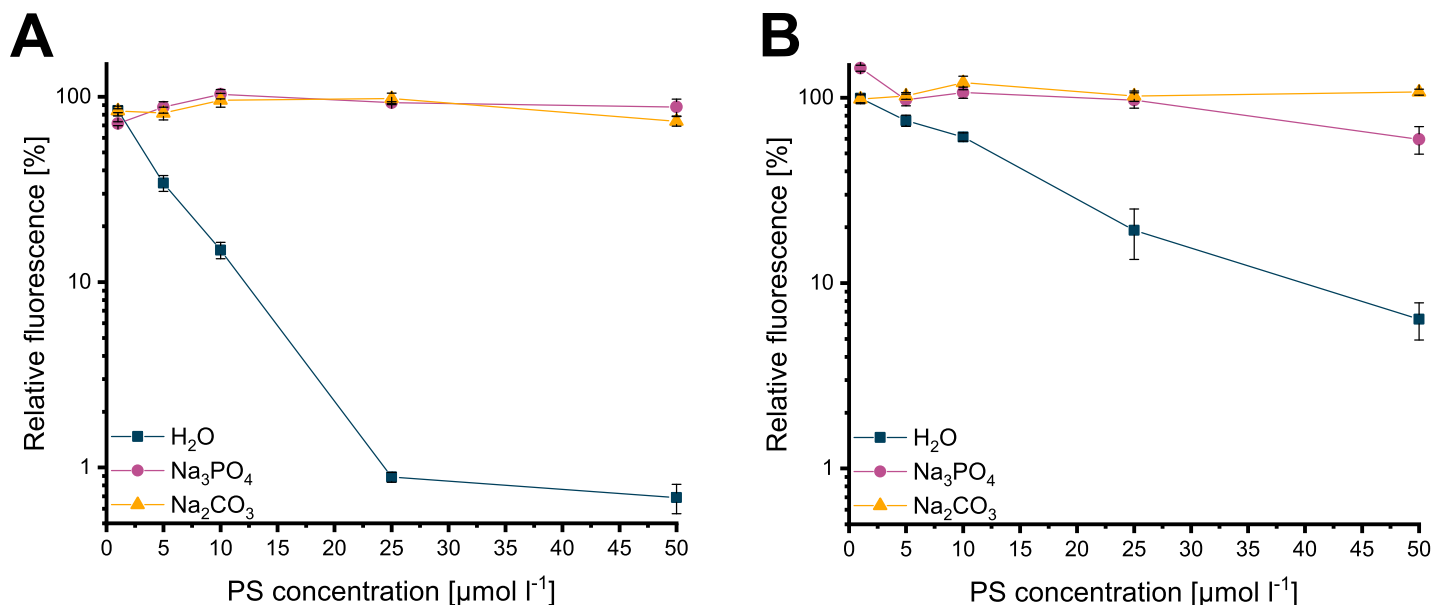


Fig 4. Results for the DPBF assays. Relative fluorescence in presence of FLASH-02a is shown in (A) and FLASH-06a in (B) after 10 s of irradiation. Different colors of the lines and symbols indicate the used environment. In this experiment, 75 mmol l⁻¹ of sodium phosphate or sodium carbonate were applied. Y axes indicate the relative fluorescence in percent referenced to the DPBF control, X axes indicate the PS concentration in μmol l⁻¹. Error bars display the calculated standard deviation of the triplicates.

<https://doi.org/10.1371/journal.pone.0253212.g004>

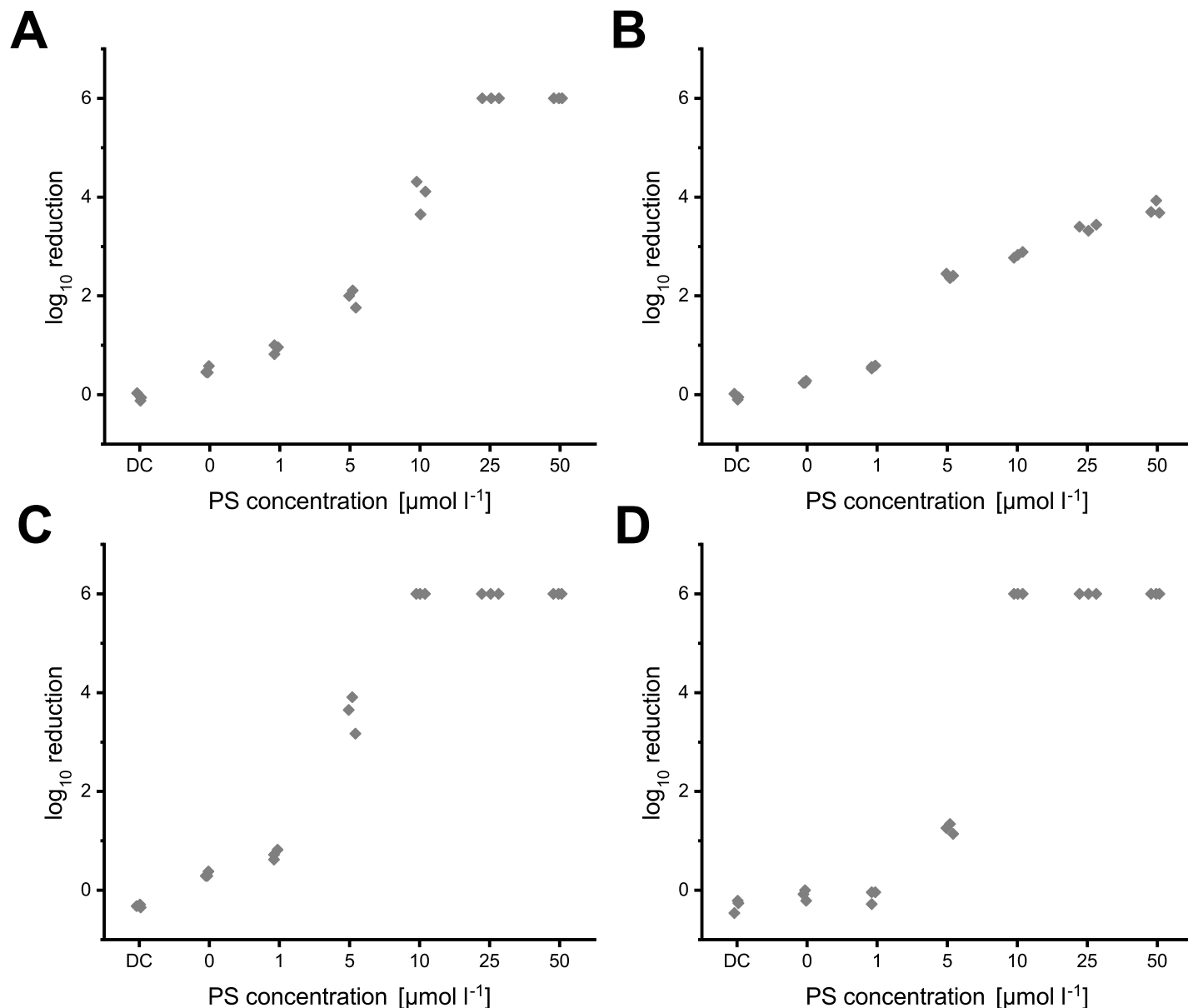


Fig 5. Results for the photodynamic inactivation without the application of ions. Logarithmic reduction values of *S. aureus* with FLASH-02a (A) and FLASH-06a (B) compared to the logarithmic reduction of *P. aeruginosa* treated with FLASH-02a (C) and FLASH-06a (D). Y axis of the graphs indicate the decadic logarithmic reduction while the x axis displays the different concentrations of the applied PS with DC indicating the dark control (no irradiation, 50 μmol l⁻¹ PS). As each experiment was carried out by n = 3, each dot represents one single value from a single experiment.

<https://doi.org/10.1371/journal.pone.0253212.g005>

FLASH-06a was less efficient in the inactivation of bacterial cells, for *S. aureus* the inactivation did not exceed four orders of magnitude (Fig 5B). However, besides the treatment of *S. aureus* with FLASH-06a, both bacteria could be inactivated to the lower limit of detection of six orders of magnitudes. Each obtained logarithmic reduction value for each experiment is displayed in the S4 Dataset. All tested conditions diverge significantly from each other except for concentrations of FLASH-06a below 5 μmol l⁻¹ for *P. aeruginosa*. Detailed statistics are given in S2 File.

When comparing the photodynamic inactivation for *S. aureus* in H₂O, sodium carbonate and sodium phosphate, dark control (DC), light control (0 μmol l⁻¹) and 1 μmol l⁻¹ of any PS, no noteworthy reduction of the number of viable bacterial cells was obtained. Even with

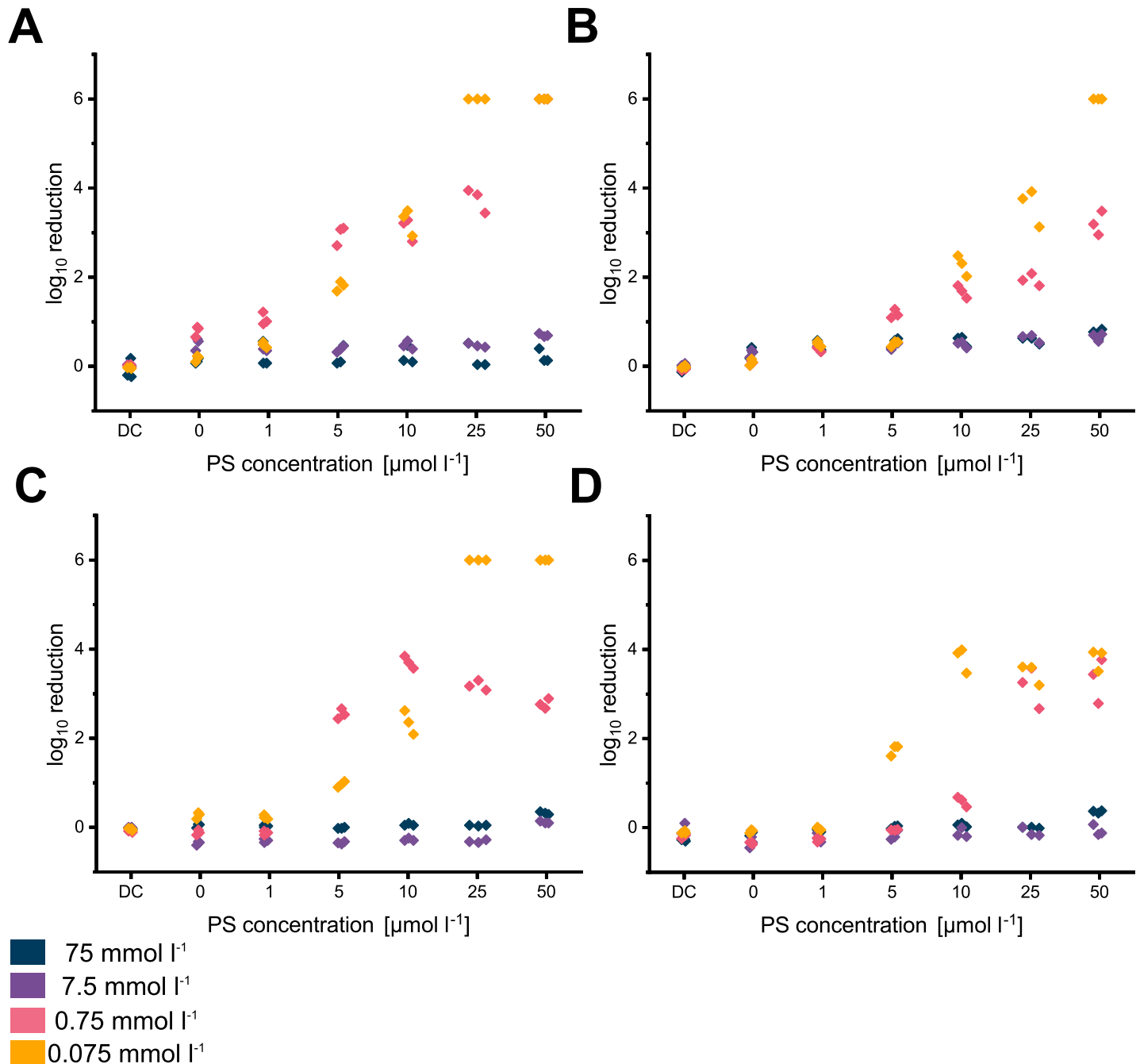


Fig 6. Logarithmic inactivation for *S. aureus* data obtained for each experiment displayed as scatter plot. (A) shows results for sodium phosphate and FLASH-02a, (B) displays the results for sodium carbonate and FLASH-02a. Obtained values for FLASH-06a are displayed in (C) for sodium phosphate and (D) for sodium carbonate. Y axes indicate the decadic logarithmic reduction and x axes indicate the PS concentration in $\mu\text{mol l}^{-1}$ or the dark control (DC). Different colors of the dots indicate the various sodium carbonate or sodium phosphate concentrations.

<https://doi.org/10.1371/journal.pone.0253212.g006>

increasing PS concentrations up to $50 \mu\text{mol l}^{-1}$, no efficient inactivation was achieved for 75 and 7.5 mmol l^{-1} of the ions at the constant light exposure of 0.72 J cm^{-2} (40 s of irradiation).

Only if concentrations of sodium phosphate were reduced to at least 0.75 mmol l^{-1} and $5 \mu\text{mol l}^{-1}$ of FLASH-02a (Fig 6A) or FLASH-06a (Fig 6C), logarithmic reduction started to

exceed one order of magnitude. For sodium carbonate and FLASH-02a, this critical point was reached for $10 \mu\text{mol l}^{-1}$ of respective PS with 0.75 mmol l^{-1} of sodium carbonate. Therefore, PDI had a better efficiency with phosphate, while carbonate seemed to have a much more detrimental effect on the system (Fig 6A and 6C vs. Fig 6B and 6D). For *S. aureus*, the best inactivation results were obtained when ion concentrations were as low as possible with PS concentrations from 25 to $50 \mu\text{mol l}^{-1}$. A statistical analysis of the logarithmic reduction values of the various applied conditions is given in S3 File. Measured logarithmic reduction values for each experiment are displayed in the S5 Dataset.

The observations were quite similar for the Gram-negative organism *P. aeruginosa*. H_2O , sodium carbonate and sodium phosphate did not lead to a reduction of the dark control (DC), light control ($0 \mu\text{mol l}^{-1}$) and $1 \mu\text{mol l}^{-1}$ exceeding one order of magnitude. Again, increasing PS concentrations did not result in an efficient inactivation exceeding three orders of magnitude for 75 and 7.5 mmol l^{-1} of both tested solutions. In contrast to the results obtained for *S. aureus*, the Gram-negative strain was eradicated with more than 6 orders of magnitude for $0.075 \text{ mmol l}^{-1}$ of sodium phosphate (Fig 7A and 7C) with PS concentrations as low as $10 \mu\text{mol l}^{-1}$. The results of the statistical analysis of the obtained logarithmic reduction values for *P. aeruginosa* are included in S4 File. Inactivation of *P. aeruginosa* in the presence of sodium carbonate was less efficient than for sodium phosphate which was in good agreement with results obtained for *S. aureus* (Fig 7B and 7D). In general, inactivation with FLASH-02a was more efficient (Figs 6A, 6B, 7A and 7B) than with FLASH-06a (Figs 6C, 6D, 7C and 7D). Measured logarithmic reduction values for each experiment are deposited in the S6 Dataset.

Additionally, the presence of carbonates and phosphates did not alter the binding behavior of the PS in a detrimental manner, the amount of PS attached to bacterial cells did either not diverge significantly from the H_2O control or was in some cases significantly higher when ionic solutions were applied. The results of a statistical analysis are included in S5 File. The mean calculated amounts and the corresponding standard deviation of bound PS to the respective cells are shown in Table 1. The results of each measurement are included in the S7 Dataset.

Discussion

The results of the present investigation show some obstacles as ions like carbonate and phosphate can hamper PDI of flavin PS. Ions in combination with the herein used PS change the mechanism in chemical, physical and biological manners.

The spectra without ions showed a photobleaching effect that was more pronounced for FLASH-06a compared to FLASH-02a, most likely due to the chemical nature of the molecules due to larger side chains of FLASH-06a. Degradation effects without involvement of ions have been described for other flavins previously [32,33].

However, the presented study showed that phosphate and carbonate react by a light-based mechanism with the used flavin PS altering the chemical structure. Time dependent spectra showed isosbestic points under addition of carbonate and phosphate. Isosbestic points in general are strong hints at mass conservation, indicating a variety of compounds, most likely even the involvement of just two substances [34].

Even though all ion treated PS with isosbestic points meet the requirement according to the definition of Thomas and Burgess [27] the isosbestic points are not sharp and clearly defined in a strict sense. Shifts in isosbestic points are either caused by different molar extinction coefficients due to the experimental condition or the contribution of a third, unknown substance [35], experimentally shown by Harris and Bashford [36].

It is known that riboflavin derivatives undergo chemical changes upon light irradiation, resulting in several isosbestic points in the absorption spectra [37–39]. We tentatively assume

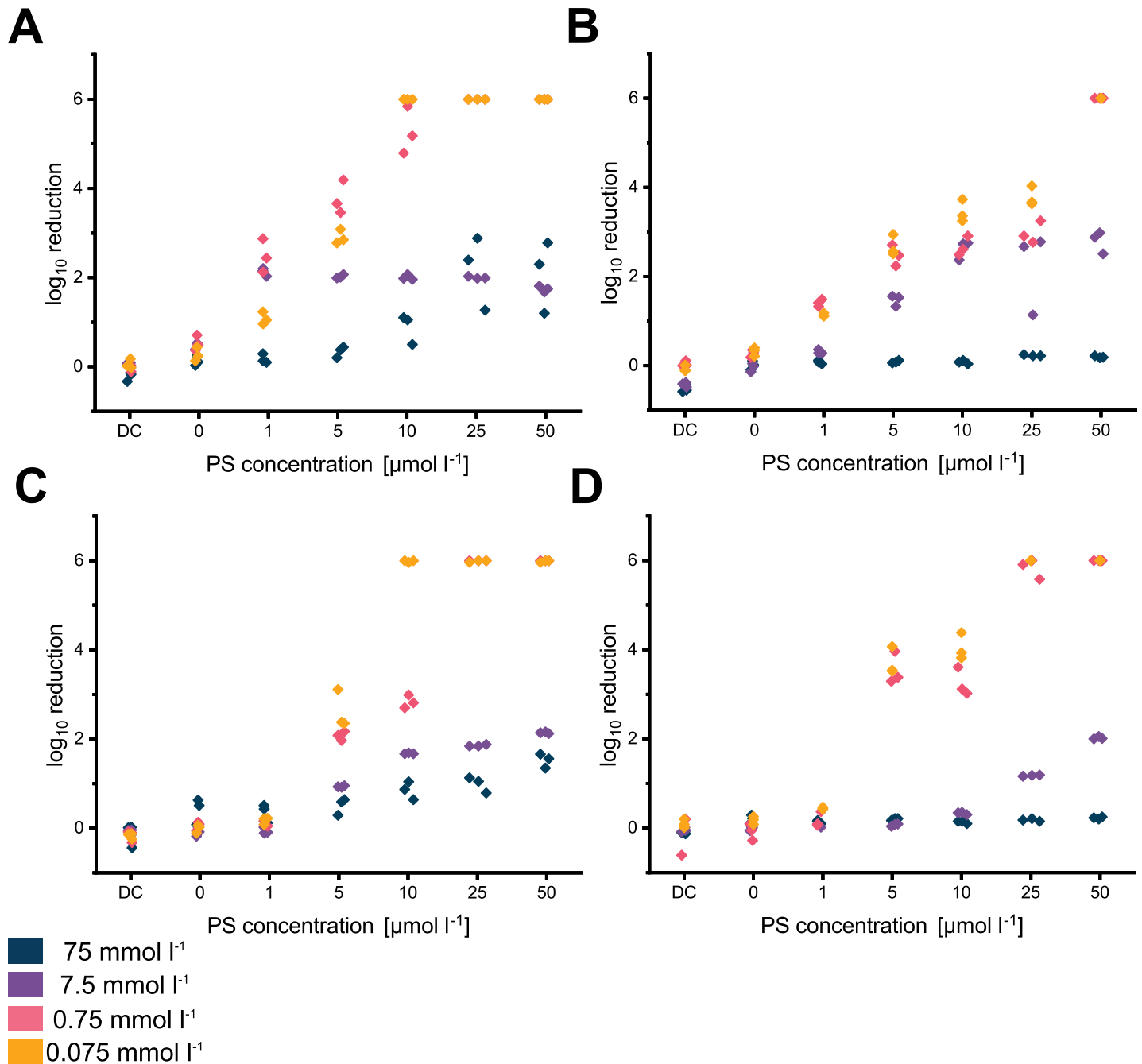


Fig 7. Logarithmic inactivation for *P. aeruginosa* data obtained for each experiment displayed as scatter plot. (A) shows results for sodium phosphate and FLASH-02a, (B) displays the results for sodium carbonate and FLASH-02a. Obtained values for FLASH-06a are displayed in (C) for sodium phosphate and (D) for sodium carbonate. Y axes indicate the decadic logarithmic reduction and x axes indicate the PS concentration in $\mu\text{mol l}^{-1}$ or the dark control (DC). Different colors of the dots indicate the various sodium carbonate or sodium phosphate concentrations.

<https://doi.org/10.1371/journal.pone.0253212.g007>

that degradation of FLASH-02a in the presence of phosphate occurs via cleavage of the side chain to lumichrome [32] possibly followed by an unspecific degradation as observed for example in dairy products [40]. However, for carbonate the transmission spectra are quite distinct from the ones of phosphate, indicating the involvement of more than one substance.

Table 1. Results of the binding assays.

PS	Ions	c (salt) [mmol l ⁻¹]	c(PS) bound to <i>S. aureus</i> [μmol l ⁻¹]	Standard deviation	c(PS) bound to <i>P. aeruginosa</i> [μmol l ⁻¹]	Standard deviation
FLASH-02a	H ₂ O		31.29	0.91	30.90	0.29
	Na ₂ CO ₃	75	31.77	1.72	28.51	1.09
	Na ₂ CO ₃	0.075	33.11	1.41	35.40	0.66
	Na ₃ PO ₄	75	31.39	0.35	39.68	0.50
	Na ₃ PO ₄	0.075	32.67	1.38	35.60	0.42
FLASH-06a	H ₂ O		25.76	1.02	27.71	1.13
	Na ₂ CO ₃	75	27.53	1.41	28.29	0.49
	Na ₂ CO ₃	0.075	29.11	0.98	29.96	0.75
	Na ₃ PO ₄	75	28.12	1.01	27.64	1.93
	Na ₃ PO ₄	0.075	29.76	0.97	31.28	0.32

<https://doi.org/10.1371/journal.pone.0253212.t001>

Therefore, it is speculated that in this specific case after the side chain cleavage additionally to lumichrome lumiflavin is produced. Neither of the both assumed molecules are capable of producing singlet oxygen. Organisms encounter such degradation products on a daily basis without being harmed, as shown for example for human keratinocytes where no [18] or very low [22] toxicity was found. Although the structural discussion of FLASH-02a is more of a speculative nature, FLASH-06a presents with a clearer situation. It is hypothesized that the ester bonds of the side chains are at least partially hydrolyzed. The remaining scaffold of the former PS might then undergo a cyclization comparable to cyclodehydroriboflavin CDRF—similar to the photoaddition of riboflavin [32,41]. It has been described elsewhere that both carbonate and phosphate facilitate such processes [41]. However, carbonate promotes the cyclisation more than phosphate, which is also supported by the data shown in this publication. The work of Vaid *et al.* shows that the cyclization of riboflavin is depending on the ionic concentration of are in good consistency with the results presented here. The proposed CDRF-like end product is just as lumichrome or lumiflavin no longer capable of producing singlet oxygen as it was observed in this study by DPBF assays. Again, we observed a less detrimental effect of phosphate for singlet oxygen production compared to carbonate which is also supported by work from other researchers [41].

Additionally, this publication may impact PDI in general as well. Ubiquitous ions as well as other small molecules are frequently present when PDI is applied outside a laboratory setting. These substances may initiate photochemical reactions of the PS leading to the usage of the absorbed light energy for chemical reactions rather than for singlet oxygen production. Such effects decrease the efficacy of killing bacteria as shown here for flavin PS by reducing the amount of generated singlet oxygen. However, e.g. Kainz *et al.* demonstrated the formation of zinc(II)-cyclen-flavin complexes in combination with Fe/C nanoparticles [42]. The use of such methods could protect flavins from harmful effects caused by ions.

It is crucial to understand how ions influence PDI since a major aim is the application of photodynamic inactivation in environments outside the laboratory. Future fields of application include the treatment of wastewater [43,44], the disinfection of drinking water [45,46], decontamination of food [47], the reduction of the bacterial load on surfaces [48] or the decolonization of skin [49]. However, ions are not only included in environmental photodynamic inactivation, but sometimes even *in vitro* studies often use phosphate buffered saline or culture medium for PDI experiments that contain various ions or inhibitory substances [50–52]. Tap water or wastewater may contain various ions like Na⁺, Ca²⁺, Mg²⁺, and HCO₃⁻ with a concentration to a few mmol l⁻¹, whereas these ions can also be found on animal or human skin, in particular HCO₃⁻ with concentrations of up to 4 mmol l⁻¹ [53,54].

A literature screening concerning PS concentration and applied fluence reveals divergent parameters that were chosen for efficient inactivation. On the one hand, PDI was efficient of up to four orders of magnitude at low light doses and low porphyrin PS concentrations under ambient light conditions [31]. Yang *et al.* successfully inactivated *Propionibacterium acnes* with a curcumin PS by applying 0.09 J cm^{-2} and PS concentrations as low as $1.5 \mu\text{mol l}^{-1}$ [55]. Efficient inactivation was also shown with flavin PS at a concentration of $10 \mu\text{mol l}^{-1}$ and a light exposure of 1.5 J cm^{-2} [18]. Jemli and co-workers showed an efficient reduction of five orders of magnitude by using $10 \mu\text{mol l}^{-1}$ of methylene blue, rose Bengal or TMPyP with a light dose of 0.13 J cm^{-2} in an wastewater environment [43].

On the other hand, some studies used elevated PS concentrations and/or high light exposures [56–58]. Bactericidal action in wastewater for example was achieved with different PS in the $\mu\text{mol l}^{-1}$ range at high light exposures up to a few hundred J cm^{-2} [43,45,59]. Carvalho *et al.* studied the application of PDI in the context of wastewater treatment, achieving a logarithmic reduction of three orders of magnitude. The study used a porphyrin PS at a concentration as low as $5 \mu\text{mol l}^{-1}$ and a light dose of 145.8 J cm^{-2} [44].

A review article [60] listed 19 animal studies in which bacteria were treated in wounded skin using different PS. It is striking that the light exposure shows high values ranging from $6\text{--}423 \text{ J cm}^{-2}$ with a mean value of 163 J cm^{-2} . Another study showed the difference of *in vitro* and *in vivo* application of PDI. When using a cationic Zn(II) phthalocyanine PS, MRSA was efficiently inactivated *in vitro* using PS concentrations of less than $1 \mu\text{mol l}^{-1}$ and a 48 J cm^{-2} light exposure [61]. For inactivation of MRSA in an animal wound model *in vivo* the authors had to increase PS concentration to $7.8 \mu\text{mol l}^{-1}$ and light exposure to about 300 J cm^{-2} . Another research group showed the inactivation of clinically relevant organisms with polycationic PS in nutrient broth. Possibly due to inhibitory substances in the culture medium, light doses of up to 40 J cm^{-2} had to be applied [56].

In a publication concerning a phenalenone PS, organisms with importance in dentistry like *Enterococcus faecalis*, *Actinomyces naeslundii* or *Fusobacterium nucleatum* were efficiently inactivated. These experiments were carried out in PBS buffer with PS concentrations of $100 \mu\text{mol l}^{-1}$ and light doses of 72 J cm^{-2} [57]. Another study used quite similar organisms and PS in concentrations of up to $250 \mu\text{mol l}^{-1}$ applying light doses of up to 150 J cm^{-2} [58].

Therefore, the major problem behind these studies is that all used different PS, bacteria, PS concentrations, light sources, light irradiance and light doses. Although some adaptations are necessary when using different photosensitizers or bacteria, it is obvious that there are further elements impacting PDI. Higher light exposure and PS concentrations might be applied to counteract detrimental effects of various substances that are inevitably present in environmental settings. Four studies also assumed a connection between the presence of inhibitory substances and reduced inactivation efficacy [62–65]. Besides only inhibitory effects there are also enhancing substances known such as EDTA [65], sodium azide [66] and potassium iodine [67,68].

Conclusion

The success of PDI as a new treatment against pathogens requires a successful application beyond standardized laboratory experiments. The impact of ubiquitous ions on the photodynamic mechanism may complicate the application under environmental conditions. As shown in this study, carbonate and phosphate alter the chemical structure of the PS leading to less singlet oxygen generation and hence reduced inactivation of bacteria. The lower the amount of additional material in PDI and the higher the applied light dose is, the better the inactivation. This study provides practical advice for future studies with flavin PS in the presence of phosphate and carbonate. Furthermore, this study stresses the inevitable importance of chemical

analysis, physical measurements and investigations concerning bacterial inactivation prior to the application outside the laboratory.

Supporting information

S1 Dataset. Transmission values for FLASH-02a.

(XLSX)

S2 Dataset. Transmission values for FLASH-06a.

(XLSX)

S3 Dataset. Relative fluorescence values of each conducted DPBF assay with calculated standard deviation.

(XLSX)

S4 Dataset. Logarithmic reduction values of each experiment for the tested organisms in H₂O.

(XLSX)

S5 Dataset. Logarithmic reduction values of each experiment for *S. aureus* in ionic solutions.

(XLSX)

S6 Dataset. Logarithmic reduction values of each experiment for *P. aeruginosa* in ionic solutions.

(XLSX)

S7 Dataset. Concentration measurements of attached PS to bacterial cells.

(XLSX)

S1 File. Statistical analysis of DPBF assays.

(PDF)

S2 File. Statistical analysis of inactivation data without ions.

(PDF)

S3 File. Statistical analysis of *Staphylococcus aureus* inactivation data.

(PDF)

S4 File. Statistical analysis of *Pseudomonas aeruginosa* inactivation data.

(PDF)

S5 File. Statistical analysis of binding assay data.

(PDF)

Acknowledgments

We thank G. Gmeinwieser and E. Kowalewski for their great technical assistance and D. Grohmann, L. Dengler and A. Böllmann for fruitful discussions.

Author Contributions

Conceptualization: Daniel Bernhard Eckl, Stefanie Susanne Eben, Anja Eichner, Wolfgang Bäuml, Harald Huber.

Formal analysis: Daniel Bernhard Eckl, Wolfgang Bäuml, Harald Huber.

Funding acquisition: Wolfgang Bäuml, Harald Huber.

Investigation: Daniel Bernhard Eckl, Stefanie Susanne Eben, Laura Schottenhaml, Anja Eichner.

Methodology: Daniel Bernhard Eckl, Anja Eichner.

Project administration: Wolfgang Bäuml, Harald Huber.

Supervision: Anja Eichner, Wolfgang Bäuml, Harald Huber.

Validation: Daniel Bernhard Eckl, Stefanie Susanne Eben, Laura Schottenhaml, Anja Eichner, Rudolf Vasold, Wolfgang Bäuml, Harald Huber.

Visualization: Daniel Bernhard Eckl.

Writing – original draft: Daniel Bernhard Eckl, Stefanie Susanne Eben, Wolfgang Bäuml.

Writing – review & editing: Stefanie Susanne Eben, Laura Schottenhaml, Anja Eichner, Rudolf Vasold, Andreas Späth, Wolfgang Bäuml, Harald Huber.

References

1. Gadda G. Flavins. In: Roberts CKG, editor. Encyclopedia of Biophysics. Berlin: Springer; 2013. pp. 771–771.
2. Massey V. The chemical and biological versatility of riboflavin. Biochemical Society Transactions. 2000. pp. 283–296. <https://doi.org/10.1042/bst0280283> PMID: 10961912
3. Bundesministerium für Gesundheit. Verordnung über die Zulassung von Zusatzstoffen zu Lebensmitteln zu technologischen Zwecken (Zusatzstoff-Zulassungsverordnung—ZZuLV). Bundesgesetzblatt 1998.
4. Blyth AW. LVI.—The composition of cows' milk in health and disease. Journal of the Chemical Society. 1879. pp. 530–539. <https://doi.org/10.1039/CT8793500530>
5. Mansoorabadi SO, Thibodeaux CJ, Liu HW. The diverse roles of flavin coenzymes—Nature's most versatile thespians. Journal of Organic Chemistry. 2007. pp. 6329–6342. <https://doi.org/10.1021/jo0703092> PMID: 17580897
6. Ohnishi T. Iron-sulfur clusters/semiquinones in Complex I. Biochim Biophys Acta—Bioenerg. 1998; 1364: 186–206. [https://doi.org/10.1016/s0005-2728\(98\)00027-9](https://doi.org/10.1016/s0005-2728(98)00027-9) PMID: 9593887
7. Engebrecht J, Neelson K, Silverman M. Bacterial bioluminescence: Isolation and genetic analysis of functions from *Vibrio fischeri*. Cell. 1983; 32: 773–781. [https://doi.org/10.1016/0092-8674\(83\)90063-6](https://doi.org/10.1016/0092-8674(83)90063-6) PMID: 6831560
8. Galston AW. Riboflavin-sensitized photooxidation of indoleacetic acid and related compounds. Proc Natl Acad Sci U S A. 1949; 35: 10–17. <https://doi.org/10.1073/pnas.35.1.10>
9. Posthuma J, Berends W. Triplet-triplet transfer as a mechanism of a photodynamic reaction. BBA—Biochim Biophys Acta. 1960; 41: 538–541. [https://doi.org/10.1016/0006-3002\(60\)90058-5](https://doi.org/10.1016/0006-3002(60)90058-5) PMID: 14434410
10. Chacon JN, McLearie J, Sinclair RS. Singlet oxygen yields and radical contributions in the dye-sensitized photo-oxidation in methanol of esters of polyunsaturated fatty acids (oleic, linoleic, linolenic and arachnidonic). Photochem Photobiol. 1988; 47: 647–656. <https://doi.org/10.1111/j.1751-1097.1988.tb02760.x> PMID: 2841703
11. Eichler M, Lavi R, Shainberg A, Lubart R. Flavins are source of visible-light-induced free radical formation in cells. Lasers Surg Med. 2005; 37: 314–319. <https://doi.org/10.1002/lsm.20239> PMID: 16196041
12. Bäuml W, Regensburger J, Knak A, Felgenträger A, Maisch T. UVA and endogenous photosensitizers—The detection of singlet oxygen by its luminescence. Photochemical and Photobiological Sciences. 2012. pp. 107–117. <https://doi.org/10.1039/c1pp05142c> PMID: 21986813
13. Regensburger J, Knak A, Maisch T, Landthaler M, Bäuml W. Fatty acids and vitamins generate singlet oxygen under UVB irradiation. Exp Dermatol. 2012; 21: 135–139. <https://doi.org/10.1111/j.1600-0625.2011.01414.x> PMID: 22229443
14. Baier J, Maisch T, Maier M, Engel E, Landthaler M, Bäuml W. Singlet oxygen generation by UVA light exposure of endogenous photosensitizers. Biophys J. 2006; 91: 1452–1459. <https://doi.org/10.1529/biophysj.106.082388> PMID: 16751234

15. Remucal CK, McNeill K. Photosensitized amino acid degradation in the presence of riboflavin and its derivatives. *Environ Sci Technol*. 2011; 45: 5230–5237. <https://doi.org/10.1021/es200411a> PMID: [21591753](https://pubmed.ncbi.nlm.nih.gov/21591753/)
16. Kashiwabuchi RT, Khan Y, Carvalho FRDS, Hirai F, Campos MS, McDonnell PJ. Antimicrobial susceptibility of photodynamic therapy (UVA/riboflavin) against *Staphylococcus aureus*. *Arq Bras Oftalmol*. 2012; 75: 423–426. <https://doi.org/10.1590/s0004-27492012000600011> PMID: [23715147](https://pubmed.ncbi.nlm.nih.gov/23715147/)
17. Thakuri PS, Joshi R, Basnet S, Pandey S, Taulale SD, Mishra N. Antibacterial photodynamic therapy on *Staphylococcus aureus* and *Pseudomonas aeruginosa in-vitro*. *Nepal Med Coll J*. 2011; 13: 281–284. PMID: [23016481](https://pubmed.ncbi.nlm.nih.gov/23016481/)
18. Maisch T, Eichner A, Späth A, Gollmer A, König B, Regensburger J, et al. Fast and effective photodynamic inactivation of multiresistant bacteria by cationic riboflavin derivatives. *PLoS One*. 2014; 9: e111792. <https://doi.org/10.1371/journal.pone.0111792> PMID: [25469700](https://pubmed.ncbi.nlm.nih.gov/25469700/)
19. Maisch T. Strategies to optimize photosensitizers for photodynamic inactivation of bacteria. *J Photochem Photobiol B Biol*. 2015; 150: 2–10. <https://doi.org/10.1016/j.jphotobiol.2015.05.010> PMID: [26048255](https://pubmed.ncbi.nlm.nih.gov/26048255/)
20. Castano AP, Demidova TN, Hamblin MR. Mechanisms in photodynamic therapy: Part one—Photosensitizers, photochemistry and cellular localization. *Photodiagnosis and Photodynamic Therapy*. 2004. pp. 279–293. [https://doi.org/10.1016/S1572-1000\(05\)00007-4](https://doi.org/10.1016/S1572-1000(05)00007-4) PMID: [25048432](https://pubmed.ncbi.nlm.nih.gov/25048432/)
21. Maisch T, Baier J, Franz B, Maier M, Landthaler M, Szeimies R-M, et al. The role of singlet oxygen and oxygen concentration in photodynamic inactivation of bacteria. *Proc Natl Acad Sci U S A*. 2007; 104: 7223–7228. <https://doi.org/10.1073/pnas.0611328104> PMID: [17431036](https://pubmed.ncbi.nlm.nih.gov/17431036/)
22. Eichner A, Gollmer A, Späth A, Bäuml W, Regensburger J, König B, et al. Fast and effective inactivation of *Bacillus atrophaeus* endospores using light-activated derivatives of vitamin B2. *Photochem Photobiol Sci*. 2015; 14: 387–396. <https://doi.org/10.1039/c4pp00285g> PMID: [25423452](https://pubmed.ncbi.nlm.nih.gov/25423452/)
23. Morrison PWJ, Connon CJ, Khutoryanskiy V V. Cyclodextrin-mediated enhancement of riboflavin solubility and corneal permeability. *Mol Pharm*. 2013; 10: 756–762. <https://doi.org/10.1021/mp3005963> PMID: [23294178](https://pubmed.ncbi.nlm.nih.gov/23294178/)
24. Schoenen J, Jacqy J, Lenaerts M. Effectiveness of high-dose riboflavin in migraine prophylaxis: A randomized controlled trial. *Neurology*. 1998; 50: 466–470. <https://doi.org/10.1212/wnl.50.2.466> PMID: [9484373](https://pubmed.ncbi.nlm.nih.gov/9484373/)
25. Mueller JH, Hinton J. A Protein-Free Medium for Primary Isolation of the *Gonoecoccus* and *Meningococcus*. *Proc Soc Exp Biol Med*. 1941; 48: 330–33. <https://doi.org/10.3181/00379727-48-13311>
26. Bäuml W, Maisch T, Späth A. 10H-benzo[g]pteridine-2,4-dione derivatives, method for the production thereof, and use thereof. WO2012/175729 A1, 2012.
27. Thomas O, Cerda V. From Spectra to Qualitative and Quantitative Results. In: Thomas O, Burgess C, editors. *UV-Visible Spectrophotometry of Water and Wastewater*. Amsterdam: Elsevier B.V.; 2007. pp. 31–33.
28. Eckl DB, Huber H, Bäuml W. First Report on Photodynamic Inactivation of Archaea Including a Novel Method for High-Throughput Reduction Measurement. *Photochem Photobiol*. 2020; 96: 883–889. <https://doi.org/10.1111/php.13229> PMID: [32073658](https://pubmed.ncbi.nlm.nih.gov/32073658/)
29. Bechert T, Steinrücke P, Guggenbichler JP. A new method for screening anti-infective biomaterials. *Nature Medicine*. 2000. pp. 1053–1056. <https://doi.org/10.1038/79568> PMID: [10973328](https://pubmed.ncbi.nlm.nih.gov/10973328/)
30. Fabritius M, Al-Munajjed AA, Freytag C, Jülke H, Zehe M, Lemarchand T, et al. Antimicrobial silver multilayer coating for prevention of bacterial colonization of orthopedic implants. *Materials (Basel)*. 2020;13. <https://doi.org/10.3390/ma13061415> PMID: [32245004](https://pubmed.ncbi.nlm.nih.gov/32245004/)
31. Eckl DB, Dengler L, Nemmert M, Eichner A, Bäuml W, Huber H. A Closer Look at Dark Toxicity of the Photosensitizer TMPyP in Bacteria. *Photochem Photobiol*. 2018; 94: 165–172. <https://doi.org/10.1111/php.12846> PMID: [28940456](https://pubmed.ncbi.nlm.nih.gov/28940456/)
32. Ahmad I, Vaid FHM. Photochemistry of Flavins in Aqueous and Organic Solvents. In: Silva E, Edwards AM, editors. *Flavins: Photochemistry and Photobiology*. Cambridge: RSC Publishing; 2007. pp. 13–40. <https://doi.org/10.1039/9781847555397-00013>
33. Ahmad I, Fasihullah Q, Vaid FHM. A study of simultaneous photolysis and photoaddition reactions of riboflavin in aqueous solution. *J Photochem Photobiol B Biol*. 2004; 75: 13–20. <https://doi.org/10.1016/j.jphotobiol.2004.04.001> PMID: [15246345](https://pubmed.ncbi.nlm.nih.gov/15246345/)
34. Gallot S, Thomas O. Fast and easy interpretation of a set of absorption spectra: theory and qualitative applications for UV examination of waters and wastewaters. *Fresenius J Anal Chem*. 1993. <https://doi.org/10.1007/BF00322762>
35. Berlett BS, Levine RL, Stadtman ER. Use of isosbestic point wavelength shifts to estimate the fraction of a precursor that is converted to a given product. *Anal Biochem*. 2000. <https://doi.org/10.1006/abio.2000.4876> PMID: [11112281](https://pubmed.ncbi.nlm.nih.gov/11112281/)

36. Poole RK, Bashford CL. Spectrophotometry and Spectrofluorimetry: A Practical Approach. Harris DA, Bashford CL, editors. Oxford: IRL Press; 1987.
37. Penzkofer A. Reduction-oxidation photocycle dynamics of flavins in starch films. *Int J Mol Sci*. 2012. <https://doi.org/10.3390/ijms13079157> PMID: 22942758
38. Kottke T, Heberle J, Hehn D, Dick B, Hegemann P. Phot-LOV1: Photocycle of a blue-light receptor domain from the green alga *Chlamydomonas reinhardtii*. *Biophys J*. 2003. [https://doi.org/10.1016/S0006-3495\(03\)74933-9](https://doi.org/10.1016/S0006-3495(03)74933-9) PMID: 12547798
39. Song SH, Dick B, Penzkofer A, Hegemann P. Photo-reduction of flavin mononucleotide to semiquinone form in LOV domain mutants of blue-light receptor phot from *Chlamydomonas reinhardtii*. *J Photochem Photobiol B Biol*. 2007. <https://doi.org/10.1016/j.jphotobiol.2006.12.007> PMID: 17292618
40. Tagliaferri E, Bosset JO, Eberhard P, Bütikofer U, Sieber R. Untersuchung einiger Kriterien zum Nachweis von Veränderungen der Vollmilch nach thermischen und mechanischen Behandlungen sowie nach verschiedenen langen Belichtungszeiten. II: Bestimmung des Vitamins B1 mit Hilfe einer neuentwickelten RP-HPLC-Methode. *Mitteilungen aus dem Gebiete der Leb und Hyg*. 1992; 83: 435–452.
41. Vaid FHM, Gul W, Faiyaz A, Anwar Z, Ejaz MA, Zahid S, et al. Divalent anion catalyzed photodegradation of riboflavin: A kinetic study. *J Photochem Photobiol A Chem*. 2019; 371: 59–66. <https://doi.org/10.1016/j.jphotochem.2018.10.048>
42. Kainz QM, Späth A, Weiss S, Michl TD, Schätz A, Stark WJ, et al. Magnetic Nanobeads as Support for Zinc(II)-Cyclen Complexes: Selective and Reversible Extraction of Riboflavin. *ChemistryOpen*. 2012; 1: 125–129. <https://doi.org/10.1002/open.201200008> PMID: 24551499
43. Jemli M, Alouini Z, Sabbahi S, Gueddari M. Destruction of fecal bacteria in wastewater by three photosensitizers. *J Environ Monit*. 2002; 4: 511–516. <https://doi.org/10.1039/b204637g> PMID: 12195992
44. Carvalho CMB, Gomes ATPC, Fernandes SCD, Prata ACB, Almeida MA, Cunha MA, et al. Photoinactivation of bacteria in wastewater by porphyrins: Bacterial β -galactosidase activity and leucine-uptake as methods to monitor the process. *J Photochem Photobiol B Biol*. 2007; 88: 112–118. <https://doi.org/10.1016/j.jphotobiol.2007.04.015> PMID: 17616398
45. Kuznetsova NA, Makarov DA, Kaliya OL, Vorozhtsov GN. Photosensitized oxidation by dioxygen as the base for drinking water disinfection. *J Hazard Mater*. 2007; 146: 487–491. <https://doi.org/10.1016/j.jhazmat.2007.04.064> PMID: 17532568
46. Jori G, Magaraggia M, Fabris C, Soncin M, Camerin M, Tallandini L, et al. Photodynamic inactivation of microbial pathogens: Disinfection of water and prevention of water-borne diseases. *J Environ Pathol Toxicol Oncol*. 2011; 30: 261–271. <https://doi.org/10.1615/jenvironpatholtoxicoloncol.v30.i3.90> PMID: 22126619
47. Glueck M, Schamberger B, Eckl P, Plaetzer K. New horizons in microbiological food safety: Photodynamic Decontamination based on a curcumin derivative. *Photochem Photobiol Sci*. 2017; 16: 1784–1791. <https://doi.org/10.1039/c7pp00165g> PMID: 29105723
48. Eichner A, Holzmann T, Eckl DB, Zeman F, Koller M, Huber M, et al. Novel photodynamic coatings reduce the bioburden on near-patient surface thereby reducing the risk for onward pathogen transmission—a field study in two hospitals. *J Hosp Infect*. 2020; 104: 85–91. <https://doi.org/10.1016/j.jhin.2019.07.016>.
49. Schreiner M, Bäuml W, Eckl D, Späth A, König B, Eichner A. MRSA decolonization of human skin via photodynamic treatment. *Br J Dermatol*. 2018; 179: e242–e242. <https://doi.org/10.1111/bjd.17287>
50. Engelhardt V, Krammer B, Plaetzer K. Antibacterial photodynamic therapy using water-soluble formulations of hypericin or mTHPC is effective in inactivation of *Staphylococcus aureus*. *Photochem Photobiol Sci*. 2010; 9: 365–369. <https://doi.org/10.1039/b9pp00144a> PMID: 20221463
51. Lambrechts SAG, Aalders MCG, Van Marle J. Mechanistic study of the photodynamic inactivation of *Candida albicans* by a cationic porphyrin. *Antimicrob Agents Chemother*. 2005; 49: 2026–2034. <https://doi.org/10.1128/AAC.49.5.2026-2034.2005> PMID: 15855528
52. Tavares A, Carvalho CMB, Faustino MA, Neves MGPM, Tomé JPC, Tomé AC, et al. Antimicrobial photodynamic therapy: Study of bacterial recovery viability and potential development of resistance after treatment. *Mar Drugs*. 2010; 8: 91–105. <https://doi.org/10.3390/md8010091> PMID: 20161973
53. Sato K, Kang WH, Saga K, Sato KT. Biology of sweat glands and their disorders. I. Normal sweat gland function. *J Am Acad Dermatol*. 1989; 20: 537–563. [https://doi.org/10.1016/s0190-9622\(89\)70063-3](https://doi.org/10.1016/s0190-9622(89)70063-3) PMID: 2654204
54. Patterson MJ, Galloway SDR, Nimmo MA. Variations in regional sweat composition in normal human males. *Exp Physiol*. 2000; 85: 869–875. <https://doi.org/10.1111/j.1469-445x.2000.02058.x> PMID: 11187982
55. Yang MY, Chang KC, Chen LY, Hu A. Low-dose blue light irradiation enhances the antimicrobial activities of curcumin against *Propionibacterium acnes*. *J Photochem Photobiol B Biol*. 2018; 189: 21–28. <https://doi.org/10.1016/j.jphotobiol.2018.09.021> PMID: 30273795

56. Hamblin MR. Polycationic photosensitizer conjugates: effects of chain length and Gram classification on the photodynamic inactivation of bacteria. *J Antimicrob Chemother.* 2002; 49: 941–951. <https://doi.org/10.1093/jac/dkf053> PMID: 12039886
57. Cieplik F, Späth A, Regensburger J, Gollmer A, Tabenski L, Hiller KA, et al. Photodynamic biofilm inactivation by SAPYR—An exclusive singlet oxygen photosensitizer. *Free Radic Biol Med.* 2013; 65: 477–487. <https://doi.org/10.1016/j.freeradbiomed.2013.07.031> PMID: 23891675
58. Späth A, Leibl C, Cieplik F, Lehner K, Regensburger J, Hiller KA, et al. Improving photodynamic inactivation of bacteria in dentistry: Highly effective and fast killing of oral key pathogens with novel tooth-colored type-II photosensitizers. *J Med Chem.* 2014; 57: 5157–5168. <https://doi.org/10.1021/jm4019492> PMID: 24884918
59. Almeida J, Tomé JPC, Neves MGPMS, Tomé AC, Cavaleiro JAS, Cunha Â, et al. Photodynamic inactivation of multidrug-resistant bacteria in hospital wastewaters: Influence of residual antibiotics. *Photochem Photobiol Sci.* 2014; 13: 626–633. <https://doi.org/10.1039/c3pp50195g> PMID: 24519439
60. Sun Y, Ogawa R, Xiao BH, Feng YX, Wu Y, Chen LH, et al. Antimicrobial photodynamic therapy in skin wound healing: A systematic review of animal studies. *Int Wound J.* 2020; 17: 285–299. <https://doi.org/10.1111/iwj.13269> PMID: 31724831
61. Dharmaratne P, Wang B, Wong RCH, Chan BCL, Lau KM, Ke MR, et al. Monosubstituted tricationic Zn (II) phthalocyanine enhances antimicrobial photodynamic inactivation (aPDI) of methicillin-resistant *Staphylococcus aureus* (MRSA) and cytotoxicity evaluation for topical applications: *in vitro* and *in vivo*. *Emerg Microbes Infect.* 2020; 1–29. <https://doi.org/10.1080/22221751.2019.1699450> PMID: 31859589
62. Bhavya ML, Umesh Hebbar H. Efficacy of blue LED in microbial inactivation: Effect of photosensitization and process parameters. *Int J Food Microbiol.* 2019; 290: 296–304. <https://doi.org/10.1016/j.ijfoodmicro.2018.10.021> PMID: 30414562
63. Glueck M, Hamminger C, Fefer M, Liu J, Plaetzer K. Save the crop: Photodynamic Inactivation of plant pathogens I: Bacteria. *Photochem Photobiol Sci.* 2019; 18: 1700–1708. <https://doi.org/10.1039/c9pp00128j> PMID: 31214675
64. Gsponer NS, Spesia MB, Durantini EN. Effects of divalent cations, EDTA and chitosan on the uptake and photoinactivation of *Escherichia coli* mediated by cationic and anionic porphyrins. *Photodiagnosis Photodyn Ther.* 2015; 12: 67–75. <https://doi.org/10.1016/j.pdpdt.2014.12.004> PMID: 25560416
65. Galstyan A, Dobrindt U. Determining and unravelling origins of reduced photoinactivation efficacy of bacteria in milk. *J Photochem Photobiol B Biol.* 2019; 197. <https://doi.org/10.1016/j.jphotobiol.2019.111554> PMID: 31326843
66. Huang L, St. Denis TG, Xuan Y, Huang YY, Tanaka M, Zadlo A, et al. Paradoxical potentiation of methylene blue-mediated antimicrobial photodynamic inactivation by sodium azide: Role of ambient oxygen and azide radicals. *Free Radic Biol Med.* 2012; 53: 2062–2071. <https://doi.org/10.1016/j.freeradbiomed.2012.09.006> PMID: 23044264
67. Huang L, Szewczyk G, Sarna T, Hamblin MR. Potassium Iodide Potentiates Broad-Spectrum Antimicrobial Photodynamic Inactivation Using Photofrin. *ACS Infect Dis.* 2017; 3: 320–328. <https://doi.org/10.1021/acsinfectdis.7b00004> PMID: 28207234
68. Yuan L, Lyu P, Huang YY, Du N, Qi W, Hamblin MR, et al. Potassium iodide enhances the photobactericidal effect of methylene blue on *Enterococcus faecalis* as planktonic cells and as biofilm infection in teeth. *J Photochem Photobiol B Biol.* 2020; 203: 111730. <https://doi.org/10.1016/j.jphotobiol.2019.111730>